Proceedings of HT2005
2005 ASME Summer Heat Transfer Conference
July 17-22, 2005, San Francisco, California, USA

HT2005-72679

THERMAL CHARACTERIZATION OF DIELECTRIC AND PHASE CHANGE MATERIALS FOR THE OPTICAL RECORDING APPLICATIONS

Y. Yang, Chun-Teh Li, S. M. Sadeghipour, and M. Asheghi

Mechanical Engineering Department,
Carnegie Mellon University, Pittsburgh, PA 15213

H. Dieker and M. Wuttig

I. Physikalisches Institut der RWTH Aachen, D-52056 Aachen, Germany

Abstract

Advances in the phase change optical recording technology strongly depend on the optical and thermal optimizations of the metal/$ZnS\text{-}SiO_2$/phase change multilayer structure, which requires accurate modeling and thermal characterization of PC media structure. In the present work, the thermal conductivities of the amorphous and crystalline $Ge_4Sb_1Te_5$ (GST) phase change; and $ZnS\text{-}SiO_2$ dielectric layers of thickness in the range of 50 nm to 300 nm have been measured using the transient thermoreflectance technique. The data are between a factor of 2-4 different from the previously measured values for thin film and bulk samples. The thermal boundary resistance at metal/$ZnS\text{-}SiO_2$ interface is found to be around 7×10^{-8} m^2W^{-1}. This might have serious implications for the future phase change recording application which attempts to achieve the high writing speeds by decreasing the thickness of $ZnS\text{-}SiO_2$ dielectric layer.

I. INTRODUCTION

Phase change optical recording is a new challenging technology for the data storage comparing with the traditional magnetic recording. With the increasing use of multimedia, phase-change rewritable optical disks, e.g. CD (compact disk) and DVD (digital versatile disk), are becoming more popular. The optical PC data storage devices provide relatively short data access rates (~ 10 MHz) and moderate areal densities. As in other areas of data storage, there has been tremendous demand and pressure, driven by consumer application, for inexpensive high-density PC systems. So far, the optical data storage industry has succeeded to respond to this demand by using a combination of shorter wavelength lasers and high numerical aperture (NA) lens technologies. Several strategies such as "multilevel storage layers" [1] and "mark radial width modulation" [2] are proposed for the next generation of the high-density PC data storage devices. There have been

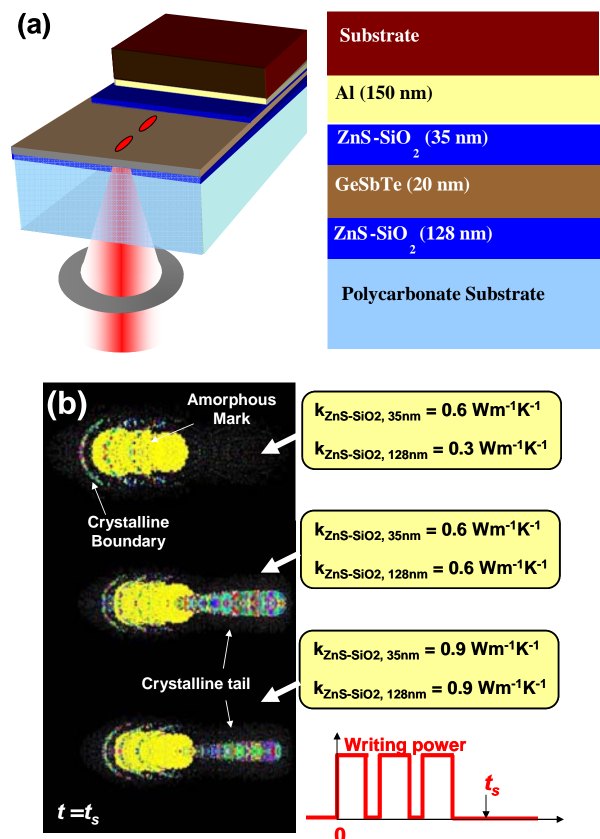

Figure 1. (a) Schematic of the phase change optical recording. (b) Effect of thermal conductivities of $ZnS\text{-}SiO_2$ dielectric layers on the simulated recording marks.

Copyright © 2005 by ASME

advances in near field optical techniques to increase density (40Gb/in^2) using solid immersion lens [3]. Hosaka *et al.* [4] (1996) demonstrated 60 nm domains in phase change media that translates to 170 Gb/in2 using a scanning near-filed optical microscope. Kado and Tohda [5] used an atomic force microscope (AFM) to locally modify the electrical property (×100) of a PC material by applying an electrical pulse between the probe and media. They achieved an areal density near 1 Tbits/cm2. The Ovonic Unified Memory (OUM), a phase-change nonvolatile semiconductor memory uses the same principle [6], however, the access to the information is provided by metal interconnects rather than AFM probe.

Phase change recording is based on the localized laser-induced heating that causes phase transition of thin film GST from crystalline to amorphous [7-10]. The typical rewritable phase change optical disk media consists of a PC layer sandwiched between two dielectric layers capped by a reflecting layer [11], as shown in Figure 1a. During recording, a focused laser pulse raises the local temperature of the storage layer to several hundred degrees Celsius, causing a phase transition from crystalline state to melt (T_{melt}). Subsequently, the molten pool cools down rapidly and forms an amorphous mark. During erasure, the local temperature is raised above the glass transition temperature, T_{glass}, and the amorphous mark is recrystallized [12]. The data retrieving is achieved by detecting the optical reflectivity difference between amorphous and crystalline states.

Great effort has been made to optimize the structure of the phase change media constituent layers in order to minimize the required laser power and write/erase times. The speed to write is limited by the thermal time constant (~ 20 ns) for cooling of the media stack while the erasure process (recrystallization) is approximately ~50ns per bit limited by the crystallization kinetics of the recording layer. The crystallization phenomenon in the phase change materials has been extensively studied [13-14]. Heat diffusion in the multilayered thin films was modeled to simulate the write, erasure and overwrite process for the PC media. Peng and Mansuripur [7] developed a theoretical model for simulating the writing and erasing processes of phase change media by taking into account temperature distributions in three dimensional space, crystallization of amorphous marks by nucleation and growth, phase transition from solid to liquid state, and formation of amorphous marks by quenching from melt. This model was further refined by introducing non-uniform computational mesh and accounting for the temperature-dependent thermal properties of PC medium [8].

Estimation of the optimum mark size, shape and quality (minimum jitter), requires extensive thermal characterization and modeling, which in turn requires accurate knowledge of the thermal conductivity and heat capacity of ZnS-SiO_2 dielectric, GST PC, and aluminum alloy reflector layers. Figure 1b shows the effect of variations in thermal conductivity of ZnS-SiO_2 dielectric layers, on the simulated recording mark size and shape. The simulation adopted finite element model (FEM) for heat conduction in PC recording media subjected to the multiple writing laser pulses [15]. The black color background represents the as-deposited amorphous GST recording layer. The bright parts are the written amorphous GST marks, surrounded by the recrystallized GST boundaries (gray shade). Detailed discussion and interpretation of the numerical results is beyond the scope of this manuscript, however, it is clear that the thermal conductivity of ZnS-SiO_2 dielectric layer can significantly influence the temperature gradient in the recording layer, which will control the extent of the recrystallization trail pattern just beyond the amorphous mark.

The heat capacity in thin film form is not usually much different from its bulk value. Thermal conductivity, however, is sensitive to the microfabrication process and therefore the microstructure, defects, impurities, voids, interfaces, and various degrees of disorder [7] as well as the thickness of the film. For instance, the ZnS-SiO_2 dielectric layer consists of nanometer-sized crystalline ZnS particles dispersed in an amorphous SiO_2 matrix. The thermal conductivity of the composite film could be very different from the bulk ZnS due to additional phonon scattering at the interfaces between two materials with different acoustic properties [16]. It was suggested the thermal conductivity could be even smaller than that of the matrix if the thermal boundary resistance between constituent components is larger than the critical boundary resistance R_c, or the size of the particles is smaller than the critical size, a_c.

A careful survey of the literature reveals that the thermal characterization techniques for optical recording media would fall into two categories. The first one, which measures the thermal properties of the PC constituent layers as part of the PC media stack, is referred as the *in-direct* method. It benefits from the usage of the existing phase-change optical recording stacks, but at the cost of developing numerical models with extensive complexity and extensive multi-parameter curve fitting. Peng and Mansuripur [7] measured the thermal conductivity of amorphous phase-change recording stacks, based on parametric fitting of constituent thin films thermal properties of the media using 3D coupled phase transformation and heat conduction simulations. A drawback of this method is the difficulty and lack of accuracy in measuring the crystallization temperature. In addition, only media stacks with amorphous phase-change layers could be tested using this approach. Recently, Meinders and Peng [17] developed a melt-threshold method for the *in situ* determination of the effective thermal conductivity of thin layers (e.g. at the crystalline state) in phase-change optical recording stacks. The method is based on the systematic variations of the thermal properties of constituent layers such that the temperature of the phase-change layer, calculated with the numerical model, matches the measured melt temperature of the phase-change material. The common shortcomings for the technique includes but not limited to (a) lack of accuracy in measurements of the incident laser power and the absorbed laser energy in successive layers (b) overall low sensitivity of the scheme due to the 3D heat spreading in the PC media stacks. Moreover, the reported thermal properties were averaged over 500°C temperature variations, which is somewhat unrealistic. The second approach, referred as *direct* method, measures the thermal conductivity of PC consistent layers by characterizing individual layers in separate experiments. Although the sample preparation effort could be considerable, it is superior to the *in-direct* method in terms of achieving high measurement sensitivity and well-defined experimental structure and thermal boundary conditions. Kim *et al.* [18] measured the thermal conductivity of amorphous and crystalline-$Ge_2Sb_2Te_5$ (GST) PC and ZnS-SiO_2 dielectric layer using 3ω method.

Recently, Meinders [19] attempted to measure the thermal conductivity of ZnS–SiO_2, and GST film material of variable thickness deposited on silicon and glass substrates using scanning thermal microscope (SThM). They concluded that while the SThM provides a tool for visualization of the thermal contrast due to changes in thermal properties with nanometer resolution, it cannot be used for accurate estimation of the thermal properties of thin layers.

 Copyright © 2005 by ASME

In this manuscript, we will report results of the normal thermal conductivity measurements of the amorphous and crystalline GST Phase change films, as well as $ZnS\text{-}SiO_2$ dielectric films of different thicknesses using the transient thermoreflectance thermometry. The thermal boundary resistances for phase change and dielectric layers are extracted by performing the measurement at different thicknesses.

II. EXPERIMENTAL PROCEDURE

A. Fabrication of the test structures

The $ZnS\text{-}SiO_2$ (ZnS-80%:SiO_2-20%) target (99.99% purity) was provided by Pioneer Materials Inc, and was used for sputtering $ZnS\text{-}SiO_2$ dielectric layers at MAT-VAC Technology Inc. fabrication facility. The thicknesses of the $ZnS\text{-}SiO_2$ dielectric layer in the measurement are 47.4nm, 95.4nm and 225nm. The amorphous $Ge_4Sb_1Te_5$ (a-GST) films with thickness of 100, 200 and 300nm were deposited on Si (100) wafers by DC magnetron sputtering using a composite target, subsequently coated with a 30nm thick SiO_2 protection layer. The film thickness was determined to by X-ray reflectometry using the Phillips X'pert MRD system. The crystalline-$Ge_4Sb_1Te_5$ (*c*-GST) films were obtained by annealing the a-GST films at 250°C for 15 min. The electrical resistivities of the amorphous and crystalline phases of the GST films were determined to be 2 and 3.1×10^{-5} Ω-m, respectively [20]. The sample preparation for the transient thermoreflectance measurement included the deposition of 500-nm-thick gold film on top of the $ZnS\text{-}SiO_2$/Silicon-substrate structure and GST/Si-substrate structure. The gold layer was chosen as top absorption layer because its thermoreflectance coefficient is relative large at red light wavelength; and its optical penetration depth is small compared to its thickness so the surface heating assumption is satisfied during the measurement.

For the electrical resistance thermometry, 500 nm thick aluminum layers were sputtered on top of $ZnS\text{-}SiO_2$ dielectric layers using Perkin-Elmer 8L sputtering machine at the nanofabrication facility at Carnegie Mellon University. Ultra high-purity argon (99.999%) was used as the sputtering gas and the pressure during sputtering was kept constant by controlling argon flow rate. In a typical run, base pressure of the system was ~ 5×10^{-3} Torr. After that, a layer of photoresist was spun on top of the sample before the lithography process. The experimental structures were patterned using GCA 4800 wafer stepper photolithography system. Aluminum bridges were etched out in commonwealth scientific ion beam etching system. In the last step the photoresist on top of metal bridges was removed in IPC barrel etcher.

B. Experimental Method

The transient thermoreflectance method employed in the present work is a non-contact, in-situ laser heating method. It has been widely used to measure thermal resistance for conduction normal to the low thermal conductivity thin films bounded metallic absorption layer and silicon substrate [21-22]. The measurements are accomplished by applying a brief pulse of laser energy at the surface of sample, and calculate the thermal conductivity from the transient temperature decay at top surface (Fig 2). A Nd:YAG laser at 532nm with ~8ns pulse and

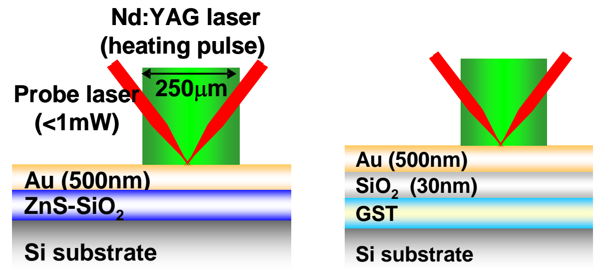

Figure 2. Thermoreflectance method for measuring out-plane thermal conductivity of $ZnS\text{-}SiO_2$ and GST thin films.

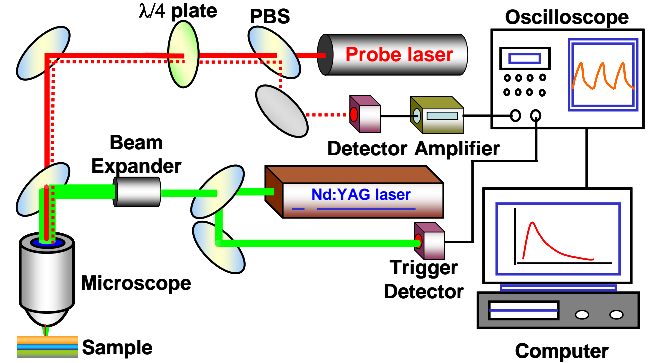

Figure 3. Schematic of the thermoreflectance setup for thermal conductivity measurement.

10Hz repetition frequency, generates a transient heat flux on the gold -coated sample. The gold layer serves two purposes, one is to absorb radiation from the pump beam, and the second is to provide the needed thermal property contrast with the measured layer. The surface temperature decay is acquired by monitoring the optical reflectivity change at 633nm from a low-power HeNe laser (Fig. 3). The probe beam is focused on sample surface to a diameter close to the diffraction limit, while the pump laser has a diameter of ~250μm, much greater than the film thickness to ensure one-dimensional heat conduction. The cubic polarization beam-splitter and quarter-wave plate are used to guide the reflected light into the PIN photodiode. The interference filter is used to prevent the pump laser radiation from leaking into the photodiode detector. The received signal is further amplified and collected by a digitizing oscilloscope with bandwidth of 500MHz and 1Gsa/s sampling rate. The measured shape of surface temperature decay is interpreted by solving the one-dimensional heat conduction equation for the given multilayer geometry under surface laser heating:

$$\frac{\partial^2 T_n}{\partial z_n^{\ 2}} = \frac{1}{\alpha_n}\frac{\partial T_n}{\partial t} \tag{1}$$

with the boundary conditions:

$$-k_{Au}\frac{\partial T}{\partial z}\Big|_{surface} = q(t), \tag{2}$$

at top surface and the following boundary conditions at the interface of consecutive layers;

 Copyright © 2005 by ASME

$$T_n\Big|_{x_n=d_n} = T_{n+1}\Big|_{x_{n+1}=0} \quad ;$$
$$k_n \frac{\partial T_n}{\partial z_n}\Big|_{x_n=d_n} = k_{n+1}\frac{\partial T_{n+1}}{\partial z_{n+1}}\Big|_{x_{n+1}=0} \qquad (3)$$

where the T_n, k_n, α_n are the temperature, thermal conductivity and diffusivity in *nth* layer; *q(t)* is the temporal profile of the heating pulse and z_n is the direction normal to the multilayer structure. The above equations for the multilayer structure was solved in time domain using the Laplace transform method. The transfer functions of the detection electronics were taken into account by measuring the shape of the heating pulse and convoluting it with the impulse response of the multilayer layer geometry. Finally, the out-of-plane thermal conductivity of the thin layer was extracted by fitting the experimental data to the solution of the equation based on the least-square method.

The uncertainty of the transient thermoreflectance measurement is relatively large, estimated to be within 20%, primarily due to the uncertainty in thickness and heat capacity of the gold layer as well as the noise in experimental data due to short-time scale of the measurement. In order to verify the results obtained from thermoreflectance method, the thermal conductivity of the ZnS-SiO_2 dielectric layers are also measured using the steady state Joule heating with electrical resistance thermometry [23-24], which has a significantly smaller uncertainty compared to the thermoreflectance technique. In this method, two parallel aluminum bridges are patterned on the ZnS-SiO_2 dielectric layer, serving as heater and thermometer, respectively. The effective normal conductivity of the ZnS-SiO_2 layer can be calculated from temperature difference between top and bottom surface of the film, which is determined from the change in electrical resistances of the top metal bridges. The uncertainty of the electrical-resistance thermometry is estimated to be 10% in the present work, primly due to the uncertainty of indirect temperature measurement at bottom surface of the dielectric layer, as well as the thickness of the dielectric layer and the dimensions of the heater bridge [25].

III. RESULT AND DISCUSSION

Fig. 4 shows the experimental data for temperature decay profiles in the ZnS-SiO_2 - on - silicon substrate structure, It is clear that the thinner ZnS-SiO_2 film has a faster temperature decay or time constant, which is consistent with the observation based on the simple RC thermal model [26]. Table 1 compares the measured apparent thermal conductivity for the ZnS-SiO_2 films at different thicknesses obtained from thermoreflectance and the electrical resistance thermometry, which shows a good agreement considering the level of uncertainty in the experimental data.

The thermal resistance, defined as ratio of film thickness over the apparent thermal conductivity, is plotted in Fig. 5. For comparison, a collection of the experimental data reported in the literature is also included in Fig. 5, which is scattered and at times inconsistent with each other and the present results. An increase of the thermal resistance with ZnS-SiO_2 layer thickness is observed for both electrical resistance thermometry and thermoreflectance results. The linear slopes for two methods are very similar, and yield nearly identical offset values when extrapolated to zero layer thickness. One should notice that the results obtained here represent the total thermal resistance R_{th} of the ZnS-SiO_2 film, which is a combination of the intrinsic

Table 1. The measured apparent thermal conductivity of ZnS-SiO_2 at room temperature (unit: $Wm^{-1}k^{-1}$)

Dielectric Layer Thickness (nm)	Steady-State	Thermoreflectance
47.7	0.41±0.03	0.44±0.08
95.4	0.54±0.04	0.57±0.09
225	0.74±0.06	0.78±0.13

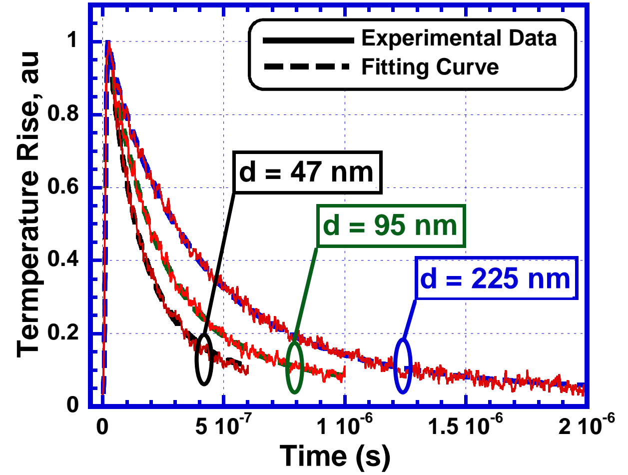

Figure 4. Transient surface temperature shape of ZnS-SiO2 layer for different thicknesses.

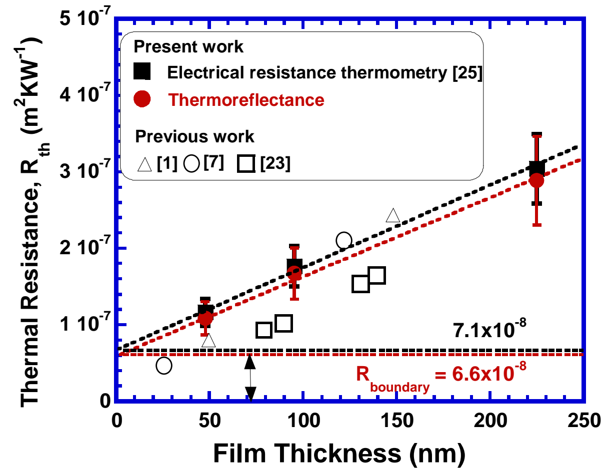

Figure 5. Measured thermal resistance for ZnS-SiO_2 film as a function of layer thickness. Experimental data extracted using *indirect* techniques are scattered and inconsistent with each other and the present data.

thermal resistance of the ZnS-SiO_2 layer $R_{ZnS\text{-}SiO2}$ and the interface thermal resistances $R_{boundary}$ between metal/ZnS-SiO_2 and ZnS-SiO_2/silicon-substrate. The $R_{boundary}$ at ZnS-SiO_2/silicon-substrate interface, maybe due to the incomplete adhesion of the ZnS-SiO_2 layer, or due to a thin interfacial layer with unusually low thermal conductivity [27]. However, the value was found to be relatively small compare to that at the metal/dioxide interface [28] and therefore is neglected in the present analysis. The $R_{boundary}$ can be extracted by extrapolating

 Copyright © 2005 by ASME

the R_{th} values to zero film thickness, under the condition that both the thermal conductivity of the ZnS-SiO_2 and $R_{boundary}$ remain independent of film thickness. The linear extrapolation to zero layer thickness yields $R_{boundary}$ of 7.0×10^{-8} m^2KW^{-1} and 6.6×10^{-8} m^2KW^{-1} for electrical resistance and thermoreflectance thermometry techniques, respectively. These data also agree with the literature values for thermal boundary resistances between metals and dielectric layers ~ 10^{-8} and 10^{-7} m^2KW^{-1} [28]. The $R_{boundary}$ between at ZnS-SiO_2/a-GST and ZnS-SiO_2/c-GST interfaces were measured by Kim *et al.* [18] to be less than 2.0×10^{-8} m^2W^{-1} and 0.6×10^{-8} m^2KW^{-1}, respectively. These values are substantially less than the $R_{boundary}$ at Al/ZnS-SiO_2 interface obtained in the present work. Therefore, the thermal boundary resistance at Al/ZnS-SiO_2 interface should receive more consideration for the practical design of phase change optical disks. It is clear that for the small thicknesses (< 100 nm), contribution of the boundary resistance to the total thermal resistance of the layer is significant. This has serious implications for the phase change recording application which will be discussed later.

Once the thickness-independent thermal resistance was fixed, the values of the intrinsic thermal conductivities of the ZnS-SiO_2 layers, can be deduced from the slopes in Fig. 5. The intrinsic thermal conductivity of the ZnS-SiO_2 film is found to be around 1.0 WmK^{-1} at room temperature and does not depend on film thickness. The thickness independent results indicate that the phonon mean free path is less than the smallest layer thickness in the measurement consistent with previous reported thermal conductivity of other oxide layers [27].

The measured intrinsic thermal conductivity ~1.0 WmK^{-1} is less than the reported values for the bulk values of ZnS single crystal ~ 17 WmK^{-1} [29] and amorphous SiO_2 ~1.23 WmK^{-1}[30]. The reduction of the thermal conductivity implies that the heat transport in the composite film might be different from that in the single amorphous film. Kim *et al.* [31] suggested that strong phonon boundary scattering in ZnS single crystal phase may be responsible for such a low thermal conductivity of the dielectric layer. The mean free path of the phonon in bulk ZnS is nearly 10 nm compared to the size of ZnS nanoparticle which is estimated to be ~2nm in radius. This yields a value of ~ 3 WmK^{-1} for the thermal conductivity of ZnS particle, which is larger than the measured value of 0.6 WmK^{-1} for 100nm thick ZnS-SiO_2 composite at room temperature [31]. The reported data are also less than the minimum thermal conductivity calculated assuming the MFP is in the order of the lattice constant [32] for ZnS and SiO_2 thin films at room temperature. Therefore, it was suggested the low thermal conductivity of ZnS-SiO_2 film is due to the phonon scattering at the interfaces between ZnS nanoparticles and the SiO_2 amorphous matrix [31].

The thermal conductivity of the particulate composites haven been theoretically studied, which depends on the particle sizes, volume fractions, shapes and the interfacial thermal contact resistance R_{Bd} between different species [16, 33-34]. The effective thermal conductivity of the composite k_{eff}, based on the effective medium theory is given by [33]:

$$\frac{k_{eff}}{k_m} = \frac{\left[k_p(1+2\alpha)+2k_m\right]+2\phi\left[k_p(1-\alpha)-k_m\right]}{\left[k_p(1+2\alpha)+2k_m\right]-\phi\left[k_p(1-\alpha)-k_m\right]} \quad (4)$$

Where k_m and k_p are the thermal conductivities of the matrix and particle, respectively; ϕ is the volume fraction of the particles. The dimensionless parameter $\alpha = k_m R_{Bd}/r$, is a

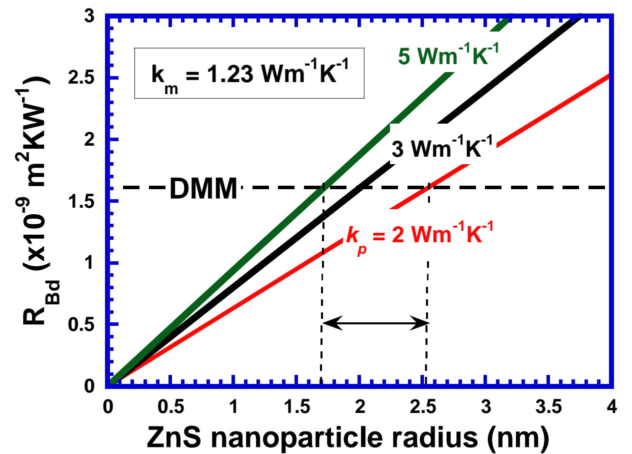

Figure 6: Comparison between the predications of Eq. (4) for the measured thermal conductivity of ZnS-SiO_2 composite. Agreement is achieved for a range of ZnS particle radius, *r*, and thermal conductivity, k_p, assuming R_{Bd}= 1.6×10^{-8} m^2KW^{-1}, which is estimated using DMM [31]. Volume fraction of the particles, ϕ = 64% [31].

measure of the influence of thermal boundary resistance on the effective thermal conductivity of the composite, where r denotes the radius of the particles. When $\alpha<<1$, the R_{Bd} is negligible and the k_{eff} lies between thermal conductivities of its constituent materials, depending on the volume fraction of the particles. When $\alpha>>1$, the R_{Bd} is dominant and the k_{eff} will be beyond the bounds of thermal conductivities of its constituent materials. The transition region occurs around $\alpha \approx 1$. Figure 6 shows a comparison between the predications of Eq. (4) for the measured thermal conductivity of ZnS-SiO_2 composite. Agreement is achieved for a range of ZnS particle radius, r, and thermal conductivity, k_p, assuming R_{Bd}= 1.6×10^{-8} m^2KW^{-1}, which is estimated using diffuse mismatch model (DMM) [31]. This is consistent with the reported ZnS particles average radius of 2 nm [31]. This translates to the value of $\alpha \sim 1$ suggesting that the thermal boundary resistances at ZnS nano-particle and SiO_2 matrix interfaces contributes to the reduction of thermal conductivity for ZnS-SiO_2 composite film. However, to fully understand the heat transport at the interfaces between ZnS nanoparticle and amorphous SiO_2 matrix, the Boltzmann transport equation (BTE) for nanoparticles dispersed in the matrix must be solved, instead of using the phenomenological models for k_m (*e.g.*, Eq.(4)) and thermal boundary resistance, R_{Bd} (e.g., DMM). This is because when the particle size is smaller than the mean path of the heat carriers, the definition of thermal conductivity and boundary resistance becomes somewhat ambigious. In this situation, the thermal resistance from the particle itself, which is particle size-dependent, is coupled with the thermal boundary resistance at ZnS and SiO_2 interface. Meanwhile, more experimental thermal conductivity data, for example at different volume fractions and ZnS particle size are required to help with a full understanding of the heat transport mechanisms in ZnS-SiO_2 composite film.

To extract the thermal conductivity of GST films, the transient temperature decay profiles are fitted to the solution of the Au/SiO_2/GST/Si substrate multilayer structure shown in Fig. 2. It is assumed that the thermal conductivity value of the top SiO_2 layer (30nm) is ~0.7 $Wm^{-1}K^{-1}$ [27], which already accounts for the contact resistance between the dielectric and Au layer. The measurements are repeated for different thicknesses of a-

Copyright © 2005 by ASME

GST and c-GST films, yielding the thickness dependent apparent thermal conductivity, which are then plotted and compared with the literature values in Fig 7. The present data for a-GST and c-GST films are consistent with those obtained from *direct* measurement approach [18], but significantly smaller than those obtained using *in-direct* measurement techniques [1,9-10]. Therefore, the *direct* measurement approach is preferred for thermal characterization of phase change media constituent layers.

It is well known that the heat transport in semiconductor is dominant by phonons, except the case where the electrical carrier concentration is relatively large, and therefore the contribution of the electrical carriers becomes appreciable. Since the carrier density for GST is order of 2×10^{20} cm^{-3}, it is worthwhile to examine the contribution of electrical carriers to the heat transport in GST films. The electron thermal conductivity of the bulk crystalline GST was calculated from the measured electrical resistivity based on the Wiedemann-Franz law, compared with the total thermal conductivity measured by photoacoustic method [35]. The percentage of the thermal conductivity due to the electrical carrier was found to be ~ 30-80% for the bulk c-GST at different tellurium concentration [35]. Based on the measured electrical resistivity for the present c-GST thin films at room temperature [20], the electron thermal conductivity is calculated to be ~0.23 Wm^{-1}K^{-1}, which is nearly 65% of the measured thermal conductivity value. One should be cautious that the Wiedemann-Franz law for calculation the electron thermal conductivity assumes the same scattering mechanism is responsible for both the thermal and electrical conductivities. In addition, the elastic electron-phonon scattering should dominate the carrier transport, which is only satisfied at temperatures well above the Debye temperature, Θ_D, or at low temperatures. Although the Wiedemann-Franz law might not hold for the GST films, the magnitude of the calculated electron thermal conductivity still suggested that the contribution of the carriers to the heat conduction can not be ignored.

IV. SUMMARY AND CONCLUSION

The thermal conductivity of ZnS-SiO_2 dielectric and phase change layer used in phase change optical recording media, are measured using the transient thermoreflectance method. The thermal boundary resistances are extracted by performing the measurement at different film thicknesses. The results of intrinsic thermal conductivity and thermal boundary resistance for ZnS-SiO_2 films agreed well with those obtained from steady state Joule heating and electrical resistance thermometry technique. The intrinsic thermal conductivity of ZnS-SiO_2 composite film is considerably less than the bulk values of ZnS and SiO_2, and is thickness independent. In addition, the thermal boundary resistance at metal/ZnS-SiO_2 interface was found to be important for the heat transport across the phase change recording media, especially for dielectric layer thickness less than 100 nm. In comparison, the heat transport in the GST film is found to be dominated by its intrinsic thermal conductivity of the layer. It is also shown that the experimental techniques that use the media stack for thermal characterization of dielectric layers can be largely in error. Therefore, it is advised that the thermal transport properties of the PC media constituent layers should be measured independently rather than as part of a media stack.

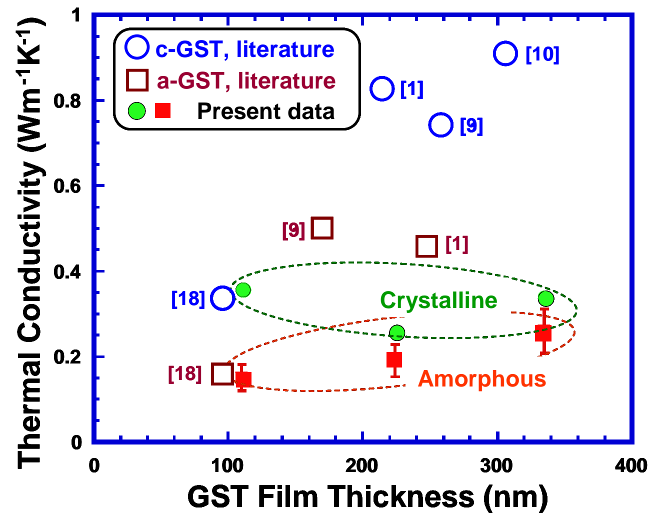

Figure 7. Measured effective thermal conductivity of a-GST and c-GST films as a function of thickness.

REFERENCES

[1] B-W. Yang, and H-P. D. Shieh, *IEEE J. Selected Topics in Quantum Electronics* 4, 821 (1998).

[2] T. Ohta, K. Nishiuchi, K. Narumi, Y. Kitaoka, H. Ishibashi, N. Yamada,and T. Kozaki, *Jpn. J. Appl. Phys. 1* 39, 700 (2000).

[3] I. Ichimura, K. Kishima,K. Osato, K. Yamamoto, Y. Kuroda, and K. Saito, , *Jpn. J. Appl. Phys. 1* 39, 962 (2000).

[4] S. Hosaka, T. Shintani, M. Miyamoto, A. Kikukawa, A. Hirotsune, M. Terao, M. Yoshida, K. Fujita, and S. Kammer, *J. Appl. Phys.* 79, 8082 (1996).

[5] H. Kado, and T. Tohda, *Jpn. J. Appl. Phys. 1* 36, 523 (1997).

[6] S. Lai and T. Lowrey, *International Electron Devices Meeting. Technical Digest* 951 (2001).

[7] C. Peng and M. Mansuripur, *Appl. Opt.* 39, 2347 (2000).

[8] A.C. Sheila and T. E. Schlesinger, *J. Appl. Phys.* 91, 2803 (2002).

[9] Y.C. Hsieh, , M. Mansuripur, , J. Volkmer, and A. Brewen, *Appl. Opt.* 36, 866 (1997).

[10] E.R. Meinders, and H.J. Borg, *Technical Digest*, ISOM 216 (2000).

[11] T. Ohta, N. Akahira, S. Ohara, and I. Satoh, *Optoelectron. Devices Technol.*10, 361 (1995).

[12] E. M. Wright, P. K. Khulbe, and M. Mansuripur, *Appl. Opt.* 39, 6695 (2000).

[13] J.H. Coombs, A. P. J. M. Jongenelis, W. Van-Es-Spiekman, and B. A. J. Jacobs, *J. Appl. Phys.* 78, 4906 (1995).

 Copyright © 2005 by ASME

[14] Z. L. Mao, H. Chen, and Ai-Lien Jung, *J. Appl. Phys.* 78, 2338 (1995).

[15] S. M. Sadeghipour, J. Reifenberg and M. Asheghi, *ASME International Mechanical Engineering Conference and R&D Exposition*, IMECE-62143, November 13-19, Anaheim, CA, USA (2004).

[16] S. Torquato and M.D. Rintoul, *Phys. Rev. Lett.* **75**, 4067 (1995).

[17] E.R. Meinders and C. Peng, *J. Appl. Phys.* 93, 3207 (2003).

[18] E. K. Kim, S. I.Kwun, S. M. Lee and H. Seo, and J.G. Yoon, *Appl. Phys. Lett.* 76, 3864 (2000).

[19] E.R. Meinders, *J. Mater. Res.* 16, 2530 (2001).

[20] D. Wamwangi, W.K. Njoroge, M. Wuttig, *Thin Solid Films* 408, 310 (2002).

[21] K. E. Goodson, O. W. Kading, M. Rosner, and R. Zachai, *J. Appl. Phys.* 66, 3134 (1995).

[22] M. N. Touzelbaev, P. Zhou, R. Venkatasubramanian, and K. E. Goodson, *J. Appl. Phys.* 90, 763 (2001).

[23] K. E. Goodson, M. I. Flik, L. T. Su, and D. A. Antoniadis, Transactions of the ASME. *Journal of Heat Transfer* 116, 317 (1994).

[24] B. Behkam, Y. Yang, and M. Asheghi, *ASME International Mechanical Engineering Conference and R&D Exposition*, November 15-21, Washington, DC., USA (2003).

[25] C-T.Li, Y. Yang, S. M. Sadeghipour, and M.Asheghi, *ASME International Mechanical Engineering Conference and R&D Exposition*, IMECE-62150, November 13-19, Anaheim, CA, USA (2004).

[26]M. N. Touzelbaev and K. E. Goodson, *Int. J. Thermophysics* 22, 243 (2001).

[27] O. W. Kading, H. Skurk, and K. E. Goodson, *Appl. Phys. Lett.* 65, 1629 (1994).

[28] E. T. Swartz and R. O. Pohl, *Appl. Phys. Lett.* 51, 2200 (1987).

[29] G.A. Slack, *Phys. Rev. B* 6, 3791 (1972).

[30] D.G. Cahill and R.O. Pohl, *Phys. Rev. B* 35, 4067 (1987).

[31] E.-K. Kim, S.-I. Kwun, S.-M. Lee, H. Seo, and J.-G. Yoon, *Phys. Rev. B* 61, 6036 (1997).

[32] D.G. Cahill and R.O. Pohl, Annu. *Rev. Phys. Chem.* 39, 93 (1988).

[33]L. C. Davis, B. E. Artz, *J. Appl. Phys.* 77, 4954 (1995).

[34] C-W. Nan, R. Birringer, D. R. Clarke, H. Gleiter, *J. Appl. Phys.* 81, 6692 (1997).

[35] J. M. Ya´n˜ez-Limo´n, J. Gonza´lez-Herna´ndez, J. J. Alvarado-Gil, I. Delgadillo, and H. Vargas, *Phys. Rev. B* 52, 16321 (1995).

Copyright © 2005 by ASME